

# Cation Effects on Rotational Dynamics of Anions and Water Molecules in Alkali ( $\text{Li}^+$ , $\text{Na}^+$ , $\text{K}^+$ , $\text{Cs}^+$ ) Thiocyanate ( $\text{SCN}^-$ ) Aqueous Solutions

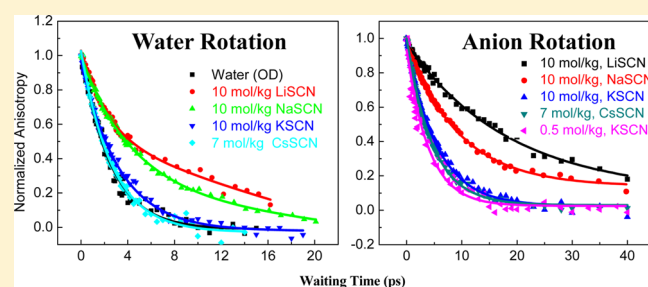
Hongtao Bian,<sup>†</sup> Hailong Chen,<sup>†</sup> Qiang Zhang,<sup>‡</sup> Jiebo Li,<sup>†</sup> Xiewen Wen,<sup>†</sup> Wei Zhuang,<sup>\*,‡</sup> and Junrong Zheng<sup>\*,†</sup>

<sup>†</sup>Department of Chemistry, Rice University, Houston, Texas 77005, United States

<sup>‡</sup>State Key Laboratory of Molecular Reaction Dynamics, Dalian Institute of Chemical Physics, Chinese Academy of Sciences, Dalian 116023, Liaoning, People's Republic of China

## Supporting Information

**ABSTRACT:** Waiting time dependent rotational anisotropies of  $\text{SCN}^-$  anions and water molecules in alkali thiocyanate ( $\text{XSCN}$ ,  $\text{X} = \text{Li}$ ,  $\text{Na}$ ,  $\text{K}$ ,  $\text{Cs}$ ) aqueous solutions at various concentrations were measured with ultrafast infrared spectroscopy. It was found that cations can significantly affect the reorientational motions of both water molecules and  $\text{SCN}^-$  anions. The dynamics are slower in a solution with a smaller cation. The reorientational time constants follow the order of  $\text{Li}^+ > \text{Na}^+ > \text{K}^+ \approx \text{Cs}^+$ . The changes of rotational time constants of  $\text{SCN}^-$  at various concentrations scale almost linearly with the changes of solution viscosity, but those of water molecules do not. In addition, the concentration-dependent amplitudes of dynamical changes are much more significant in the  $\text{Li}^+$  and  $\text{Na}^+$  solutions than those in the  $\text{K}^+$  and  $\text{Cs}^+$  solutions. Further investigations on the systems with the ultrafast vibrational energy exchange method and molecular dynamics simulations provide an explanation for the observations: the observed rotational dynamics are the balanced results of ion clustering and cation/anion/water direct interactions. In all the solutions at high concentrations ( $>5 \text{ M}$ ), substantial amounts of ions form clusters. The structural inhomogeneity in the solutions leads to distinct rotational dynamics of water and anions. The strong interactions of  $\text{Li}^+$  and  $\text{Na}^+$  because of their relatively large charge densities with water molecules and  $\text{SCN}^-$  anions, in addition to the likely geometric confinements because of ion clustering, substantially slow down the rotations of  $\text{SCN}^-$  anions and water molecules inside the ion clusters. The interactions of  $\text{K}^+$  and  $\text{Cs}^+$  with water or  $\text{SCN}^-$  are much weaker. The rotations of water molecules inside ion clusters of  $\text{K}^+$  and  $\text{Cs}^+$  solutions are not significantly different from those of other water species so that the experimentally observed rotational relaxation dynamics are only slightly affected by the ion concentrations.



## 1. INTRODUCTION

Electrolyte aqueous solutions have been important subjects in chemistry, biology, and atmospheric environment sciences and extensively investigated for many years. One of the central research issues in this field in recent years is about the correlations between ion hydrations and the resulting molecular dynamics and structures.<sup>1–7</sup> It is usually believed that anions have more pronounced effects than cations on the water structure and rotational dynamics,<sup>8,9</sup> and the effects of different anions usually follow the order of Hofmeister series,<sup>10–14</sup> e.g.,  $\text{SO}_4^{2-}$  is “structure making” and  $\text{SCN}^-$  is “structure breaking”.<sup>15–17</sup> The development of such a concept is mainly from the analyses of macroscopic properties of aqueous solutions, e.g., viscosity, surface tension, and entropy, and enthalpy of solvation measurements.<sup>17</sup> Recent experimental studies at the molecular level with ultrafast infrared lasers have revealed many novel interesting details about ion hydrations. It was found that the presence of ions does not lead to an enhancement or

breakdown of the hydrogen-bond network in liquid water.<sup>18,19</sup> Water molecules that directly interact with ions can have slower fluctuation dynamics.<sup>20–22</sup> Some anions were found to be able to significantly slow down the reorientation motions of water,<sup>5,23,24</sup> and the effects of some other anions are only very slight.<sup>18,19</sup> It was originally reported that cations were not able to affect the rotational dynamics of water,<sup>18</sup> but recent experiments began to recognize the role of cations play on the dynamics of water.<sup>25,26</sup>

In the majority of the literature about the studies of molecular dynamics in aqueous solutions with ultrafast lasers, water dynamics were typically explained in terms of ion/water direct interactions.<sup>20,27</sup> The effects of ion/ion interactions were almost completely ignored, though in the studies the ion

Received: February 16, 2013

Revised: June 9, 2013



concentrations were typically high ( $>2$  M) in the solutions where substantial amounts of ion pairing and clustering are anticipated from the predictions of MD simulations.<sup>28,29</sup> Recently, by applying the ultrafast vibrational energy exchange method,<sup>30,31</sup> we found that ions form significant amounts of clusters in MSCN ( $M = K, NH_4, Na, Cs, \text{ and } Li$ ) aqueous solutions ( $\geq 1$  M).<sup>32,33</sup> Combining vibrational energy exchange measurements with ultrafast anisotropy decay measurements, we also found that in the KSCN aqueous solutions the structural inhomogeneity because of ion clustering leads to distinct rotational dynamics of water molecules and  $SCN^-$  anions.<sup>24</sup> Adding anions of different charge densities into the KSCN solutions can dramatically change the molecular dynamics of water and  $SCN^-$  anions in very different ways.<sup>24</sup> The net changes in the dynamics were attributed to the balanced results of interactions among water, cation, and anions.<sup>24,34</sup>

The observed surprising effects of anions have led us to reexamine the somewhat controversial cation effects on the dynamics of water mentioned above.<sup>18,19,25,26</sup> In aqueous solutions of many salts at the same concentration, the viscosity of a solution with a cation of a larger charge density is typically larger, e.g., at room temperature at the concentration of 5 mol/kg (salt/water), the viscosity ratio of LiSCN, NaSCN, KSCN, and CsSCN aqueous solutions is LiSCN:NaSCN:KSCN:CsSCN = 1.85:1.48:1.05:1. The solution with the smallest cation  $Li^+$  has a viscosity 85% larger than that of the solution with the largest cation  $Cs^+$ . Based on the viscosity data and the Einstein–Stokes equation,<sup>35,36</sup> the microscopic molecular motions are expected to be slower in the solutions with cations of larger charge densities if the solutions are homogeneous. However, in concentrated aqueous solutions, ions form pairs and clusters.<sup>30,33</sup> Here, using KSCN as an example, ion pairs and clusters are defined as the assemblies of ions inside which, for any thiocyanate anion within the distance of  $\leq 4$  Å starting from the central point of its CN bond, there is at least another thiocyanate anion. 4 Å is the shortest anion distance in KSCN crystal determined with XRD measurements<sup>37</sup> and also the average anion distance in the saturated KSCN aqueous solutions estimated from the vibrational energy transfer methods described in our previous publications.<sup>30,31,33</sup> Ion clusters with different cations have slightly different critical distances as discussed in the following energy-transfer part. The definition of ion clusters does not exclude the situations that some water molecules or cations are buried inside the clusters. In fact, we believe that cations must be involved in the ion clusters to reduce the repulsions among anions though we do not have any experimental evidence to support such a hypothesis.

The structural inhomogeneity (ion pairing and clustering) does not guarantee that all species in a solution with a larger viscosity must have slower dynamics. For example, the viscosity of a 22 mol/kg KSCN aqueous solution is 2.8 times that of a 0.1 mol/kg KSCN solution. The rotation of the  $SCN^-$  anions slows down about 3 times accordingly in the concentrated solution, but that of water molecules only slightly slow down 36%.<sup>24</sup> Therefore, only from the viscosity data, it is not immediately clear whether the effect of cations on water dynamics is similar to that of the anions where a larger charge density leads to a slower rotational motion observed with the ultrafast infrared anisotropy measurements.<sup>24</sup>

In this work, we used a similar approach that was previously applied<sup>24</sup> in the studies of anion effects on the rotational

dynamics of water and  $SCN^-$  anions to investigate the cation effects in a series of MSCN ( $M = Li, Na, K, Cs$ ) aqueous solutions at room temperature: we used the ultrafast infrared anisotropy measurements to determine the rotational dynamics of both water and  $SCN^-$ , the vibrational energy exchange method to determine the ion clustering in the solutions, and molecular dynamics (MD) simulations to provide qualitative molecular pictures about the experimentally observed dynamics. From the studies, we unambiguously show that the cations can significantly affect the rotational dynamics of both water molecules and  $SCN^-$  anions in the MSCN solutions.

## 2. EXPERIMENTAL SECTION

**Experimental Methods.** The experimental setup has been described elsewhere.<sup>30,38,39</sup> Briefly, a picosecond amplifier and a femtosecond amplifier are synchronized with the same seed pulse from a Ti:sapphire oscillator. The picosecond amplifier pumps an OPA to produce 0.7–1 ps mid-IR pulses with a bandwidth  $\sim 21$   $cm^{-1}$  ( $10$ – $27$   $cm^{-1}$ ) in a tunable frequency range from 500 to 4000  $cm^{-1}$  with energy 1–40  $\mu J$ /pulse at 1 kHz. The femtosecond amplifier pumps another OPA to produce  $\sim 140$  fs mid-IR pulses with a bandwidth  $\sim 200$   $cm^{-1}$  in a tunable frequency range from 500 to 4000  $cm^{-1}$  with energy 1–40  $\mu J$ /pulse at 1 kHz. In 2D IR and pump/probe experiments, the picosecond IR pulse is the pump beam (pump power is adjusted based on need). The femtosecond IR pulse is the probe beam which is frequency resolved by a spectrograph yielding the probe axis of a 2D IR spectrum. Scanning the pump frequency yields the other axis of the spectrum. Two polarizers are added into the probe beam path to selectively measure the parallel or perpendicular polarized signal relative to the pump beam. Vibrational lifetimes are obtained from the rotation-free 1–2 transition signal  $P_{life} = P_{||} + 2 \times P_{\perp}$ , where  $P_{||}$  and  $P_{\perp}$  are parallel and perpendicular data, respectively. Rotational relaxation dynamics are acquired from the time dependent anisotropy  $R = (P_{||} - P_{\perp}) / (P_{||} + 2 \times P_{\perp})$ . In water reorientation dynamic measurements, the excitation and detection OD frequencies were set at the OD central frequency. To avoid the effect of resonance energy transfer on the anisotropy decay, HOD solutions (1 wt %  $D_2O$  in  $H_2O$ ) were used to obtain the OD reorientation dynamics in the series of XSCN ( $X = Li, Na, K, Cs$ ) aqueous solutions. In the analyses of water reorientation dynamics and vibrational energy transfer kinetics, the heat effects from the OD and thiocyanate vibrational relaxations were removed, following the procedure described in our previous publication:<sup>38</sup> the heat signal is assumed to grow with time constants slightly slower than the lifetimes of vibrational excitations of which the relaxation generates heat. The maximum amplitude of the heat signal is the transient signal at very long waiting times when most vibrational excitations have relaxed. The time-dependent heat signal calculated in this way is then subtracted from the transient signal (for both  $P_{||}$  and  $P_{\perp}$ ). Solutions in  $D_2O$  with various  $KS^{13}C^{15}N/XSCN$  ( $=2\%$ ;  $X = Li, Na, K, Cs$ ) concentrations were used to conduct the  $SCN^-$  anisotropy measurements. The validity of the approach relies on the fact that the vibrational energy exchange between  $S^{13}C^{15}N^-$  and  $SCN^-$  is much slower than the anion rotations and the resonant energy transfer among  $S^{13}C^{15}N^-$  in the solution is also much slower than rotations. As previously measured,<sup>30,31</sup> the energy-transfer time from  $SCN^-$  to  $S^{13}C^{15}N^-$  in a saturated potassium thiocyanate ( $KS^{13}C^{15}N/KSCN = 1/1$ ) aqueous solution is  $\sim 110$  ps which is slower in a more dilute solution. This value is

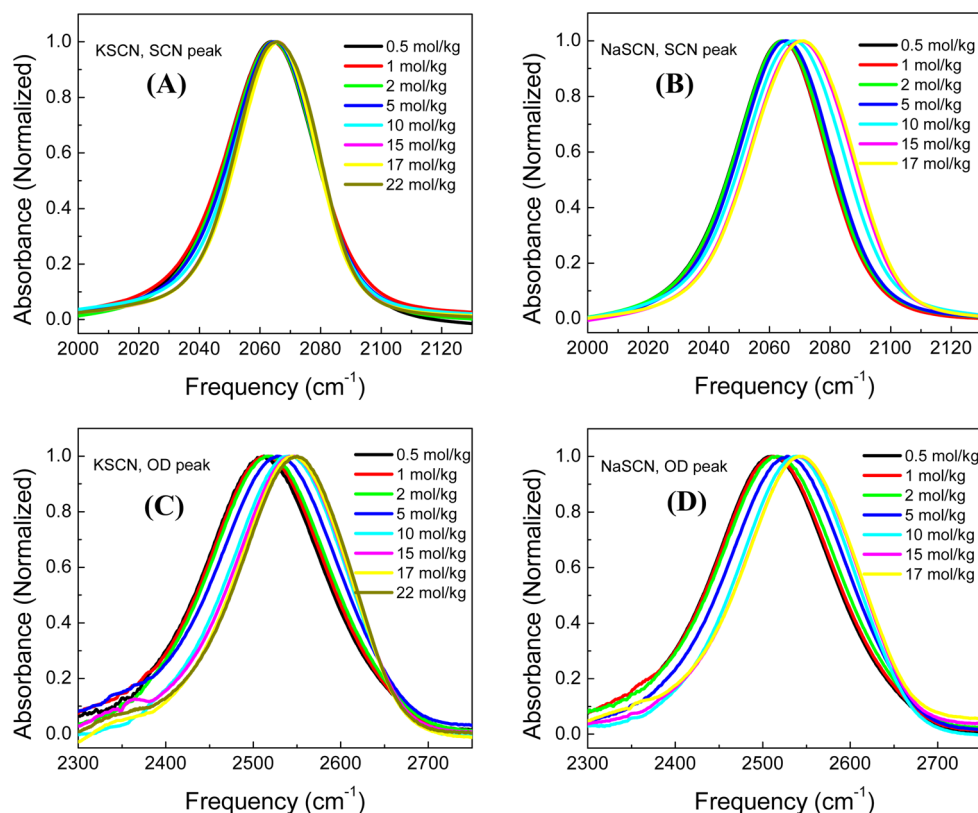


**Figure 1.** FTIR spectra of (A) KSCN and (B) NaSCN aqueous solutions ( $D_2O$ ) in the  $C\equiv N$  stretch frequency region. FTIR spectra of (C) KSCN and (D) NaSCN aqueous solution ( $HOD$ , 1 wt %  $D_2O$  in  $H_2O$ ) in the OD stretch frequency region at different concentrations. The spectra are background free. The unit of concentration is mol(MSCN)/kg(water).

significantly slower than those (faster than 30 ps) of the thiocyanate anion rotations in the solutions. The resonant energy transfer time in a pure KSCN saturated aqueous solution is 3 ps,<sup>30,31</sup> indicating that the resonant energy transfer time in the 2% sample for  $S^{13}C^{15}N^-$  will be 150 ps which is significantly slower than the rotations.

**Materials.** Unless specified, chemicals were purchased from Sigma-Aldrich and used without further purifications.  $KS^{13}C^{15}N$  was purchased from Cambridge Isotope Laboratory and used without further purification.  $D_2O$  was from C/D/N Isotopes Inc. CsSCN was synthesized by mixing  $Cs_2CO_3$  with  $NH_4SCN$  (mole ratio 1:2) in water. The solution was then heated to  $\sim 110^\circ C$  to decompose  $(NH_4)_2CO_3$  into  $CO_2$  and  $NH_3$ , which was monitored with a pH meter, and to remove the water solvent. The resulting powder was further dried in a vacuum oven at  $70^\circ C$  before use. LiSCN is highly hygroscopic. It was dried in the vacuum oven at  $70^\circ C$  with  $P_2O_5$ . The liquid samples in the FTIR and 2D IR measurements were contained in a sample cell composed of two  $CaF_2$  windows separated by a Teflon spacer. The thickness of the spacer was adjusted based on the optical densities. The experimental optical path and apparatus were purged with clean air free of  $CO_2$  or water. All the measurements were carried out at room temperature (297K).

**Molecular Dynamics Simulation Method.** The SPC/E model was adopted for the calculations of water. The parameters of KSCN and NaSCN are listed in Table S1 in the Supporting Information. In the calculations, each cubic box was filled with water molecules and ions which were inserted randomly. The numbers of water molecules and ions in the simulation boxes are listed in Table S2 in the Supporting

Information. The geometries of water molecules and  $SCN^-$  anions were kept rigid. The Lorentz–Berthelot rules were used for the combined LJ parameters. The temperature was weakly coupled to a bath with the Nose–Hoover thermostats at 298 K with the relaxation time of 0.1 ps. The weak coupling Berendsen scheme was used to control the pressure with the coupling time constant of 1 ps. The equations of motion were integrated using the leapfrog algorithm with a time step of 2 fs. The long-range Coulombic forces were treated with the Ewald summation method. The nonbonded van der Waals interactions were truncated at 12 Å using the force shifting method. Minimum image conditions were used. For each run, one 5 ns NPT ensemble equilibration was followed by a 10 ns NVE ensemble simulation used to calculate the dynamic properties. Prior to this step, several quenching simulations were carried out in order to reach equilibration for each solution. The simulation trajectories were saved every 100 fs. If the separation  $R_{X-Y}$  of atom pair X and Y is not larger than  $d$  ( $S-Ow$  ( $d = 3.6$  Å),  $N-Ow$  ( $d = 3.4$  Å),  $K-Ow$  ( $d = 3.6$  Å),  $K-S$  ( $d = 4.0$  Å),  $K-N$  ( $d = 3.5$  Å),  $Na-Ow$  ( $d = 3.2$  Å),  $Na-S$  ( $d = 3.45$  Å), and  $Na-N$  ( $d = 3.1$  Å) pairs), which corresponds to the first minimum of the RDF, they are considered as being in the first solvation shell of each other. An ion cluster is defined as following: (i) every ion X ( $X = SCN^-, Li^+, Na^+, K^+, Cs^+$ , and  $M^+$ ) is connected to at least one ion Y of the opposite charge; two ions are said to be connected if they are separated by a distance  $R_{X-Y}$  smaller than the separation  $d$  corresponding to the first minimum of the pair radial distribution function. ( $R_{X-Y} < d$  Å for  $Li-S$  ( $d = 2.75$ ),  $Li-N$  ( $d = 2.65$ ),  $Na-S$  ( $d = 3.45$ ),  $Na-N$  ( $d = 3.1$ ),  $K-S$  ( $d = 4.0$ ),  $K-N$  ( $d = 3.5$ ),  $Cs-S$  ( $d = 4.35$ ),  $Cs-N$  ( $d = 4.0$ ),  $M-S$  ( $d = 4.9$ ), and  $M-N$  ( $d = 4.55$ )).

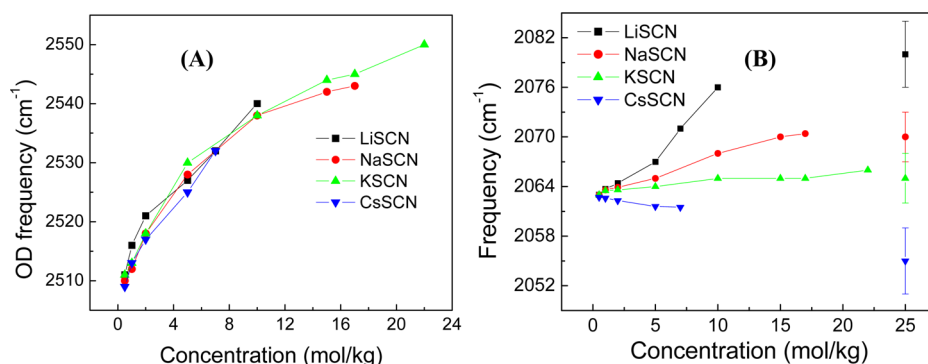


**Figure 2.** Central frequencies of (A) OD and (B) CN stretches in all MSCN aqueous solutions (MSCN, M = Li, Na, K, Cs). The frequencies at 25 mol/kg in (B) are for the molten salts.

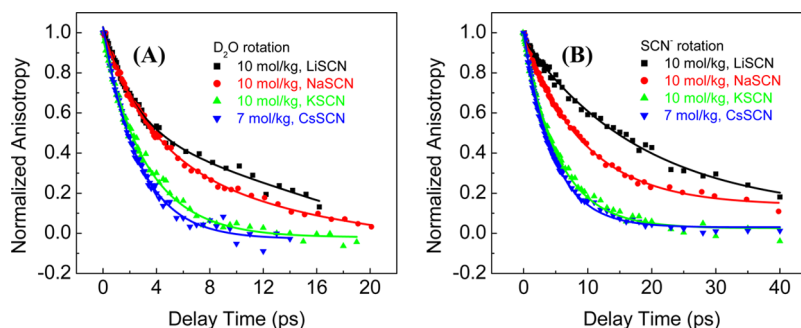


**Figure 3.** Waiting-time-dependent rotational anisotropies of (A) water molecules and (B)  $\text{SCN}^-$  in LiSCN, NaSCN, and KSCN aqueous solutions of 10 mol/kg and in a saturated CsSCN aqueous solution of 7 mol/kg.

pairs); (ii) every ion can be reached from any other ion within the assembly through a path of consecutive connections. The total number of all the ions in each ion assembly is defined as the size of the assembly. All simulations were performed with the Tinker simulation code.<sup>40</sup> The second-order reorientation correlation function  $C(t)$  of water or  $\text{SCN}^-$  ion is described as a second-order Legendre polynomial along the O–H bond direction of water and the linear vector of  $\text{SCN}^-$ .

### 3. RESULTS AND DISCUSSION

**3.1. Cation Effects on the Vibrational Frequencies of OD and CN Stretches.** Figure 1A–D shows the FTIR spectra of KSCN and NaSCN in  $\text{D}_2\text{O}$  solutions of different concentrations. In all solutions, the frequencies of both OD and CN stretches blue shift at higher ion concentrations, but the amplitudes of frequency shifts are smaller than the line widths of the peaks. Therefore, when we used lasers (with a bandwidth  $\sim 20 \text{ cm}^{-1}$ ) to excite the molecules at the central frequencies of the peaks to obtain molecular rotational dynamics, the information from the experiments is the sum information of species in different local environments, e.g., species inside ion clusters and species fully hydrated.

The OD stretch frequencies also blue shift at higher concentrations in the  $\text{Li}^+$  and  $\text{Cs}^+$  solutions. The central frequencies of OD and CN stretch peaks in all MSCN (M = Li, Na, K, Cs) aqueous solutions are plotted in Figure 2. In all MSCN aqueous solutions, the OD frequency blue shifts at higher ion concentrations (Figure 2A), and the amplitudes of frequency shifts are only dependent on the ion concentration, regardless of the nature of cations. This observation implies that the charge densities of cations do not have significant effects on the frequency of OD stretch. The observed results can be

qualitatively explained in terms of water/ion and water/water direct interactions. Because of the interactions between positive and negative charges, cations typically bind to the nonbonded electron pairs on the oxygen atoms of the water molecules. Such cation/water interactions do not directly interfere with the OD bonds of the water molecules. On the contrary, anions directly bind to the positively charged hydrogen atoms of water molecules. Such anion/water interactions directly contact the OD bond, shifting the electric field distribution and weakening the force constant of the OD stretch. Therefore, the anion effect on the OD frequency is much more significant than the cation effect. Because  $\text{SCN}^-$  is a very large anion with a low charge density, its binding to a water molecule is weaker than the water/water interactions.<sup>3,41</sup> Adding more MSCN into the solutions results in more  $\text{SCN}^-$ -associated water molecules of which the hydrogen bonds are weaker than those in bulk water, so that the OD stretch frequency shifts to higher values.

Very different from the OD frequency changes (Figure 2A), the CN frequency changes are highly dependent on the nature of cations (Figure 2B). At a very low concentration, e.g., 0.1 M, the CN stretch frequency of  $\text{SCN}^-$  in all MSCN solutions is identical ( $2063 \text{ cm}^{-1}$ ). This is because most cations are well separated from anions by water molecules. The cations are too far away to be sensed by the anions. With the increase of concentration, cations and anions become closer, and different cations begin to show different effects on the CN stretch vibrational frequency of the anion  $\text{SCN}^-$ . At higher concentrations, the CN stretch frequency in LiSCN and NaSCN solutions obviously blue shifts, it almost remains constant in the KSCN solutions, and it red shifts in the CsSCN solutions. At first glance, it seems hard to understand the different concentration-dependent cation effects, but the



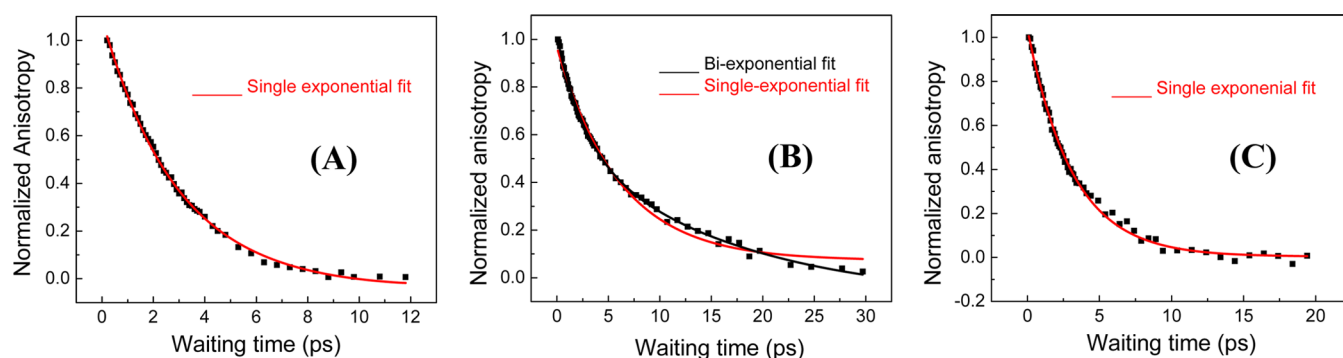
observations are explainable if we follow the idea of ion clustering. As we have measured, in MSCN ( $M = \text{Li, Na, K, Cs, NH}_4$ ) aqueous solutions of high concentrations, significant amounts of ion pairs and clusters form.<sup>30,33</sup> At higher concentrations, the sizes and concentrations of ion clusters become larger.<sup>30,33</sup> Therefore, the local environments of  $\text{SCN}^-$  anions in the aqueous solutions at higher concentrations should be closer to those of the molten salts. Accordingly, the CN stretch frequencies of  $\text{SCN}^-$  in solutions of higher concentrations should become more similar to those in the molten salts. To test this hypothesis, we summarized and listed the CN stretch frequencies of  $\text{SCN}^-$  in the molten MSCN salts from our own experiments and the literature<sup>42–44</sup> in Figure 2B at the assumed concentration of 25 mol/kg. The CN stretch frequencies are quite different in the molten salts of different cations. A higher frequency is observed for a salt with a smaller cation. It can be seen from Figure 2B that the CN frequencies of the solutions gradually approach those in the molten salts respectively with the increase of ion concentration.

**3.2. Cation Effects on the Rotational Dynamics of Water Molecules and  $\text{SCN}^-$  Anions.** As shown above, the vibrational frequency of only  $\text{SCN}^-$  anions but not water molecules is affected by the nature of cations. Differently, the rotational dynamics of both  $\text{SCN}^-$  anions and water molecules are dependent on cations. As shown in Figure 3, the rotational dynamics of both water molecules (Figure 3A) and  $\text{SCN}^-$  anions (Figure 3B) in the  $\text{Li}^+$  and  $\text{Na}^+$  solutions are obviously slower than those in the  $\text{K}^+$  and  $\text{Cs}^+$  solutions. Detailed data are listed in Table 1. In the  $\text{K}^+$  and  $\text{Cs}^+$  solutions the rotational dynamics are similar, and those in the  $\text{Li}^+$  solution are the slowest. At the concentration of 10 mol/kg, the  $\text{SCN}^-$  rotational dynamics in the NaSCN solution is a single-exponential decay with a time constant 10.2 ps, which is about 2 times that (5.3 ps) of the KSCN solution. At higher concentrations, the difference of the dynamics in the  $\text{Na}^+$  and  $\text{K}^+$  solutions becomes larger. For example, at 17 mol/kg, the  $\text{SCN}^-$  rotational time constant (25.2 ps) in the NaSCN solution is now about 3 times that (8.2 ps) of the KSCN solution. A similar trend is also observed for the water rotational motions. At the concentration of 10 mol/kg, the water rotational dynamics in the NaSCN solution can be roughly described with a single-exponential decay with a time constant 5.7 ps, which is about 1.8 times that (3.2 ps) of the KSCN solution. At higher concentrations, the difference is even larger. For example, at 17 mol/kg, the OD rotational time constant (7.6 ps for a single exponential) in the NaSCN solution is now about 2.5 times that (3.1 ps) of the KSCN solution. One apparent reason for the observed concentration-dependent cation effect is that at higher concentrations more water molecules and anions are close to cations so that the detected signal which is from all species in different local environments has more contributions from these species that are close to cations. However, the structures of these species cannot be determined or even estimated from the experimental results presented here. MD simulations which will be described later provide interesting insights about the identities of these species.

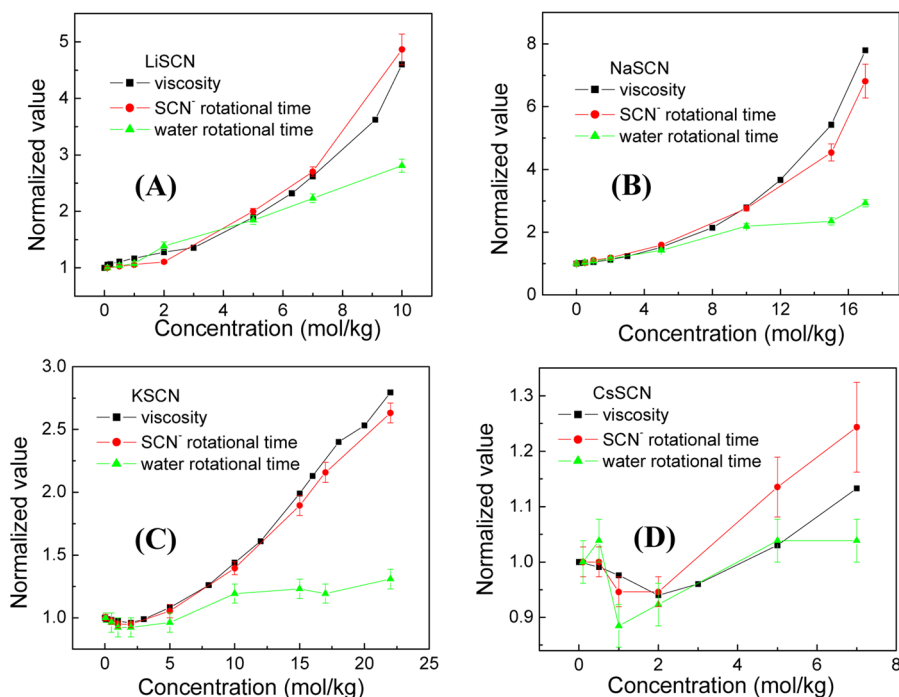
In the  $\text{K}^+$  and  $\text{Cs}^+$  solutions of all concentrations studied, the water rotational dynamics can be described well with single-exponential decays, but to describe the water dynamics in the  $\text{Na}^+$  and  $\text{Li}^+$  solutions of concentrations  $\geq 10$  mol/kg, single-exponential decays are not sufficient. Some of the data with fits of single- and biexponential decays are shown in Figure 4.

Table 1. Concentration-Dependent Rotational Time Constants of  $\text{SCN}^-$  and OD in the LiSCN, NaSCN, KSCN and CsSCN Solutions

concn (mol/kg)	LiSCN		NaSCN		KSCN		CsSCN	
	$\text{SCN}^-$ (ps)	OD (ps)	$\text{SCN}^-$ (ps)	OD (ps)	$\text{SCN}^-$ (ps)	OD (ps)	$\text{SCN}^-$ (ps)	OD (ps)
0.5	3.8 ± 0.1	2.7 ± 0.1		2.7 ± 0.1	3.8 ± 0.1	2.5 ± 0.1	3.7 ± 0.1	2.7 ± 0.1
1.0	3.9 ± 0.1	2.8 ± 0.1		2.8 ± 0.1	3.7 ± 0.1	2.4 ± 0.1	3.5 ± 0.1	2.3 ± 0.1
2.0	4.1 ± 0.2	3.6 ± 0.2		3.0 ± 0.2	3.6 ± 0.1	2.4 ± 0.1	3.5 ± 0.1	2.4 ± 0.1
5.0	7.4 ± 0.3	4.8 ± 0.3		3.7 ± 0.2	4.2 ± 0.2	2.5 ± 0.1	4.2 ± 0.3	2.7 ± 0.1
7.0	10 ± 0.4	2.6 ± 0.2 (38%) 11 ± 2.0 (62%)					4.6 ± 0.3	2.7 ± 0.1
10	18 ± 1	2.6 ± 0.2 (45%) 19.0 ± 2.0 (55%)		2.6 ± 0.6 (40%) 10.2 ± 2.0 (60%)	5.3 ± 0.2	3.1 ± 0.2		
15				2.6 ± 0.6 (40%) 17.0 ± 2.0 (60%)	7.2 ± 0.3	3.2 ± 0.2		
17				2.6 ps ± 0.6 (31%) 25.0 ± 4 (69%)	8.2 ± 0.3	3.1 ± 0.2		
22					10.0 ± 0.3	3.4 ± 0.2		



**Figure 4.** Waiting-time-dependent anisotropy decays of OD vibrational excitation signals of (A) 2 mol/kg NaSCN/water solution, (B) 15 mol/kg NaSCN/water solution, and (C) 15 mol/kg KSCN/water solution and respective single- and biexponential fits. The fitting parameters are (A) a single-exponential decay with time constant 3 ps (red line); (B) a single-exponential decay with time constant 6.1 ps (red line); a biexponential decay with time constant 2.6 ps (40%) and 17 ps (60%) (black line); and (C) a single-exponential decay with time constant 3.2 ps (red line).



**Figure 5.** Normalized viscosities,  $\text{SCN}^-$  and water (OD) rotational time constants of (A) LiSCN, (B) NaSCN, (C) KSCN, and (D) CsSCN aqueous solutions at various ion concentrations. The viscosity (0.97 cSt) of pure water is taken to be 1 for the normalization of viscosities of other solutions. The rotational time constant (2.6 ps) of pure water is taken to be 1 for the normalization of water rotations in other solutions. The rotational time constant (3.7 ps) of  $\text{SCN}^-$  in a 0.1 M MSCN solution is taken to be 1 for the normalization of  $\text{SCN}^-$  rotations in other solutions. All the rotational time constants are the time constants used in fits with single-exponential decays.

Figure 4A displays the anisotropy data of water rotation in a NaSCN solution of 2 mol/kg. The data (dots) can be described with a single-exponential decay (line) with a time constant 3.0 ps reasonably well. At a higher concentration of 15 mol/kg, the fit with a single-exponential decay with a time constant 6.1 ps (red line in Figure 4B) obviously misses the slow component of the rotational dynamics. A biexponential decay with time constants 2.6 ps (40%) and 17 ps (60%) does a much better job in describing the data (black line). At the same concentration of 15 mol/kg, a single-exponential decay with a time constant 3.2 ps (red line in Figure 4C) is sufficient to fit the water dynamics in the KSCN solution. The observations of different exponential decays in MSCN solutions are somewhat unexpected. Here, we give some tentative explanations for the phenomena. At low ion concentrations, the number of water

molecules close to cations is small. The experimental signal is mainly from those water molecules far away from cations of which the rotational time constant is close to that (2.6 ps) of bulk water, so that the anisotropy dynamics look similar to that of the bulk water—a single-exponential decay. At high ion concentrations, e.g., 10 mol/kg, where on average there is one cation for every five water molecules, substantial amounts of water molecules stay very close to cations in both NaSCN and KSCN solutions. Therefore, the experimental signal contains significant contributions from these species. Analyzing the rotational data shows that the rotations of these species in NaSCN solutions are significantly slower than that of bulk water; e.g., in the 15 mol/kg solution the slow component (60%) of the rotational decay is  $\sim 17$  ps, which is much slower than the 2.6 ps (also the fast component) of bulk water.

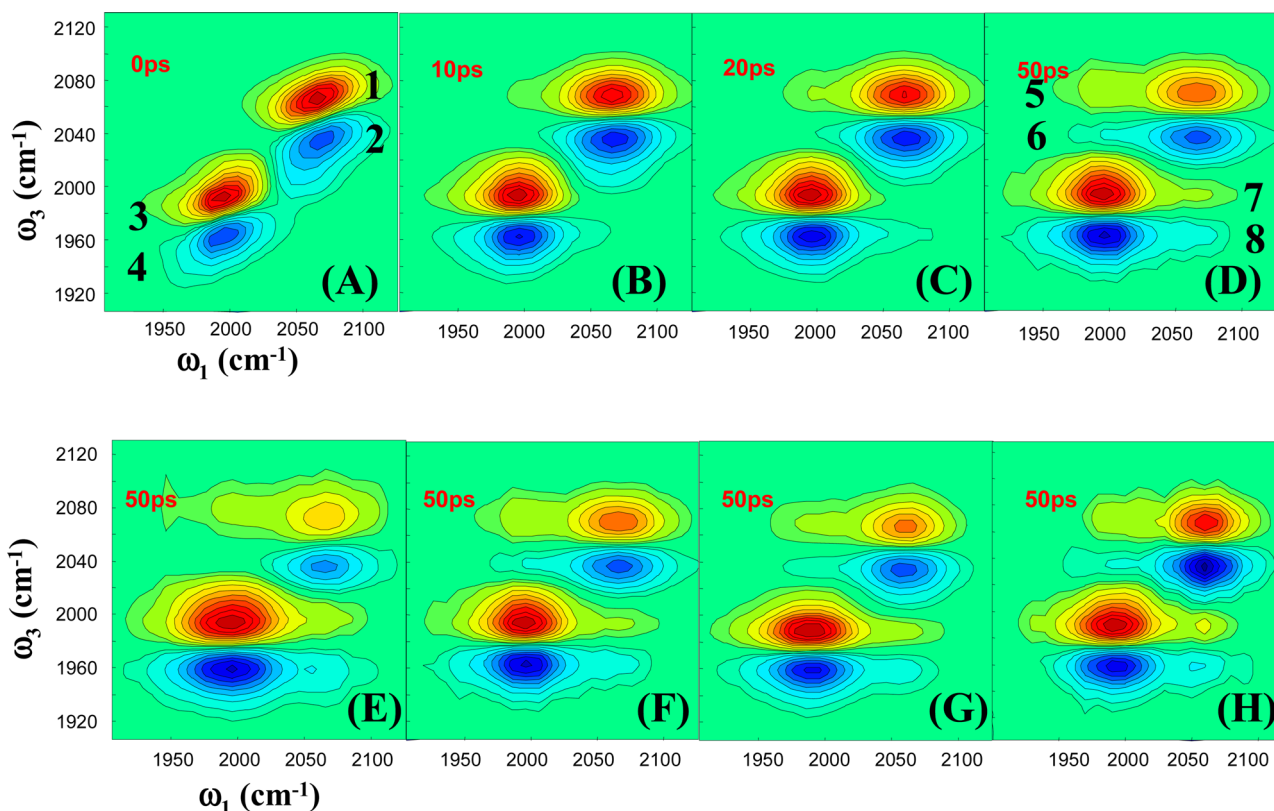


**Figure 6.** Vibrational energy exchange 2D IR spectra of MSCN/MS<sup>13</sup>C<sup>15</sup>N = 1/1 solutions at the salt concentration of 5 mol/kg at various waiting times: (A–D) the Na<sup>+</sup> solution at waiting times 0, 10, 20, and 50 ps; (E) the Li<sup>+</sup> solution at 50 ps; (F) the Na<sup>+</sup> solution at 50 ps; (G) the K<sup>+</sup> solution at 50 ps; and (H) the Cs<sup>+</sup> solution at 50 ps.

Mathematically, it is difficult to use a single-exponential decay curve to well describe the sum of two single exponentials of similar weighing but with very different time constants. Therefore, the water rotational dynamics in NaSCN solutions of high concentrations behave more like a biexponential. In the KSCN solutions, the situation is different. The rotations of those water molecules close to cations are not significantly different from that of bulk water, as implied from Figure 4C where the overall water decay constant of the KSCN solution of 15 mol/kg is only 3.2 ps which is close to that of bulk water (2.6 ps). Therefore, even if two or more water subspecies coexist in the concentrated KSCN solutions, the overall water rotational dynamics behave like a single exponential because of the similar dynamics of all subspecies. There can be another reason for the biexponential rotational decay in the concentrated NaSCN solutions. In the concentrated solutions, most of the water molecules are confined in different environments. The anisotropy decay of each confined species is not necessarily a single exponential since many coupled molecular motions besides rotations which can cause the anisotropy to decay can occur at different time scales.

Regarding the dynamical difference between the water species that are close to cations in the NaSCN and KSCN solutions, it is probably due to the different water affinities of the cations. According to the literature, the absolute hydration enthalpies of the alkali cations are −520 kJ/mol (Li<sup>+</sup>), −406 kJ/mol (Na<sup>+</sup>), −320 kJ/mol (K<sup>+</sup>), and −264 kJ/mol (Cs<sup>+</sup>), respectively.<sup>45</sup> The enthalpy values indicate that the order of water affinity is Li<sup>+</sup> > Na<sup>+</sup> > K<sup>+</sup> > Cs<sup>+</sup>. Comparing the order of enthalpy values with our rotational measurements, we find that a stronger cation/water interaction leads to a slower water

reorientation motion for the Li<sup>+</sup>, Na<sup>+</sup>, and K<sup>+</sup> solutions. This correlation is somewhat anticipated. It can come from two possible origins. One is that a stronger cation/water interaction can lead to a larger rotational free energy barrier. The other is that a stronger cation/water interaction can result in a larger ratio of cation/water pairs over cation/anion pairs. However, the correlation does not work for the K<sup>+</sup> and Cs<sup>+</sup> solutions. Water dynamics in the K<sup>+</sup> solutions are not slower than those in the Cs<sup>+</sup> solutions. In fact, they remain very similar within experimental uncertainty for all concentrations up to the CsSCN saturated concentration of 7 mol/kg, despite that the water/K<sup>+</sup> interaction is obviously stronger than the water/Cs<sup>+</sup> interaction. This exception can be explained from the water rotational times listed in Table 1. In the KSCN solutions, the water rotational dynamics are only slightly dependent on the ion concentration, implying that K<sup>+</sup> has a very weak effect on the water dynamics. Since the Cs<sup>+</sup>/water interaction is weaker than the water/K<sup>+</sup> interaction, it is possible that the perturbation of Cs<sup>+</sup> to the water dynamics is even smaller than that of K<sup>+</sup>. Therefore, the dynamics of water molecules in CsSCN solutions remain close to those in bulk water and KSCN solutions.

**3.3. Correlations between Viscosities and Rotational Dynamics.** In our previous work,<sup>24</sup> we found that the rotational dynamics of the SCN<sup>−</sup> anions and water molecules behave in very different ways in KSCN aqueous solutions of various concentrations (Figure 5C): the rotational time constants of the SCN<sup>−</sup> anions scale linearly with the change of solution viscosity (for which we do not know the exact reason and is subject to future studies), but the water dynamics are only slightly affected by the solution viscosity. Another way

to present the data to clearly show the linear and nonlinear viscosity dependences of rotations is provided in the Supporting Information (Figure S11). As shown in Figure 5, the dynamic segregation of  $\text{SCN}^-$  and water is also observed in the LiSCN (Figure 5A) and NaSCN (Figure 5B) solutions. In the CsSCN solutions (Figure 5D), even at the saturated concentration ( $\sim 7$  mol/kg), the rotation time constant of  $\text{SCN}^-$  slows down only about 20%. The dynamic segregation cannot be observed as clearly as in other solutions. Nonetheless, it can still be seen from Figure 5D that the  $\text{SCN}^-$  anions behave slightly differently from water molecules at the concentrations of 5 and 7 mol/kg.

On the basis of various control experiments in the previous work, we concluded that the rotational dynamic segregation between  $\text{SCN}^-$  anions and water molecules in KSCN solutions is because of the structural inhomogeneity in the solutions.<sup>24</sup> In other words, the dynamic segregation is the natural result of ion clustering which was experimentally observed with the vibrational energy exchange method.<sup>24,30,33</sup> By applying the vibrational energy exchange method, we also found that in other MSCN aqueous solutions substantial amounts of ions form ion clusters. It is conceivable that the dynamic segregation observed in other MSCN solutions can also be explained in terms of ion clustering in a way similar to that for the KSCN solutions.

Figure 6 displays the vibrational energy exchange spectra of MSCN/ $\text{MS}^{13}\text{C}^{15}\text{N} = 1/1$  ( $M = \text{Li}, \text{Na}, \text{K}, \text{and Cs}$ ) at the ion concentration of 5 mol/kg at various waiting times. As elaborated in our previous publications,<sup>30,31,39</sup> at 0 ps vibrational energy transfers between  $\text{SCN}^-$  and  $\text{S}^{13}\text{C}^{15}\text{N}^-$  have not occurred so that only two pairs of diagonal peaks (peaks 1–4) show up in the spectrum. Peaks 1 and 2 are the CN stretch 0–1 and 1–2 transitions, respectively, and peaks 3 and 4 are the  $^{13}\text{C}^{15}\text{N}$  stretch 0–1 and 1–2 transitions, respectively. At long waiting times, e.g., 50 ps, substantial amounts of  $\text{SCN}^-$  and  $\text{S}^{13}\text{C}^{15}\text{N}^-$  have exchanged vibrational energy, and two pairs of off-diagonal peaks (peaks 5–8) grow in. The growth of the cross peaks indicates how fast the energy transfer has occurred. In experiments, the diagonal peaks are from both isolated and clustered anions, and the off-diagonal peaks are mainly from the clustered anions because of their shorter distances. Simultaneous analyses on the growths and decays of both diagonal and off-diagonal peaks can provide us not only the energy-transfer rate constants but also the concentrations of the ion clusters. On the basis of this physical picture, we have constructed a vibrational energy exchange kinetic model.<sup>30,31</sup> Using the model, quantitative analyses (details are provided in the Supporting Information) show that in the 5 mol/kg MSCN solutions, significant amounts of the anions form clusters:  $50 \pm 4\%$  (LiSCN),  $60 \pm 4\%$  (NaSCN),  $67 \pm 4\%$  (KSCN), and  $70 \pm 4\%$  (CsSCN). Here we want to emphasize that “ion clustering” is experimentally defined by the energy-transfer rate which is determined by the relative anion distances. In the analyses, we assumed the relative anion distance ratio of the solutions to be  $r_{\text{Li}^+}:r_{\text{Na}^+}:r_{\text{K}^+}:r_{\text{Cs}^+} = 1:1.07:1.10:1.17$  based on both resonant and nonresonant energy-transfer rate constants and the vibrational energy-transfer equation and by assuming the dipole/dipole approximation if the cluster size is identical in all solutions.<sup>30,31</sup> If we assume the same anion distance (4.016 Å, the shortest CN distance in KSCN crystal)<sup>37,46</sup> and the same cluster size for all solutions, the percentages of clustered ions in all solutions from the experimental results are  $83 \pm 5\%$  (LiSCN),  $69 \pm 4\%$

(NaSCN),  $67 \pm 4\%$  (KSCN), and  $50 \pm 4\%$  (CsSCN). In both treatments, we assumed that the nature of cations does not change the refractive indices of the solutions. In crystals, the shortest distances between two CN bonds in MSCN are different. The distance is 3.91 Å in NaSCN, 4.016 Å in KSCN, and 4.8 Å in CsSCN.<sup>37,47,48</sup> The distance in LiSCN, which to our best knowledge has not been characterized, is expected to be the shortest among the MSCN salts studied here. The first treatment is to follow the trend that the CN distance is larger with a larger cation to calculate the concentrations of clusters of similar structures in different MSCN solutions. The second treatment is to calculate the concentrations of  $\text{SCN}^-$  with a fixed CN distance in all solutions. The structures of ion clusters in the second treatment can be different in different MSCN solutions because of the different sizes of cations. In the LiSCN solution,  $\text{Li}^+$  is so small that the CN distance in a structure like  $(\text{Li}^+)_m-(\text{SCN}^-)_n$  can be smaller than 4.016 Å. It is conceivable that some of the structures like  $\text{Li}^+_m(\text{H}_2\text{O})_n-(\text{SCN}^-)_k$  can have CN distances close to 4.0 Å. For the same reason, in CsSCN probably fewer CN distances are smaller than 4.0 Å because of the relatively large size of  $\text{Cs}^+$  and it is not very likely that the CN distances in the clusters can be significantly smaller than those in the crystal. It is therefore not surprising that, in the second treatment, more ion clusters form in a solution with a smaller cation. Nonetheless, both treatments of energy-transfer data suggest that considerable amounts of anions form clusters in all the MSCN solutions at the concentration of 5 mol/kg. The ion clustering results are anticipated from the observed dynamic segregation in MSCN solutions displayed in Figure 5, following our previous explanation for the dynamic segregation in KSCN solutions. However, the ion clustering percentages obtained from the experiments cannot fully explain the observed cation effects on the rotational dynamics of water molecules and anions in the MSCN solutions presented in Figure 3. Factors other than ion clustering, e.g., the direct cation/water/anion interactions, can also play important roles responsible for the cation effects.

**3.4. MD Simulations.** **3.4.1. Reorientational Dynamics of Water Molecules.** To explore factors besides ion clustering responsible for the dynamic differences in solutions with different cations, we performed MD simulations on aqueous solutions of NaSCN and KSCN. In the simulations, we can visualize species at different environments and track their dynamics. The dynamic time constant and population of each species can provide important information for us to understand the microscopic origins of the experimentally observed dynamical behaviors.

From the simulation results, we define the subspecies of water in MSCN aqueous solutions as follows: (1) *pure water* of which the first solvation shell is filled only with water molecules; (2) *cation-bound water* of which the first solvation shell has only cation(s) and water molecules; (3) *anion-bound water* of which the first solvation shell has only anion(s) and water molecules; and (4) *bridged water* of which the first solvation shell has at least one cation and one anion. Similarly, the subspecies of  $\text{SCN}^-$  ions can also be defined as follows: (1) *hydrated  $\text{SCN}^-$*  of which the first solvation shell contains only water molecules; and (2) *cation-bound  $\text{SCN}^-$*  of which the first solvation shell contains at least one cation. No other  $\text{SCN}^-$  species besides these two has been found from the simulations. We extract the rotational dynamics from the reorientation correlation function of each subspecies which is defined at  $t = 0$  regardless of its structural evolution during the accumulation of



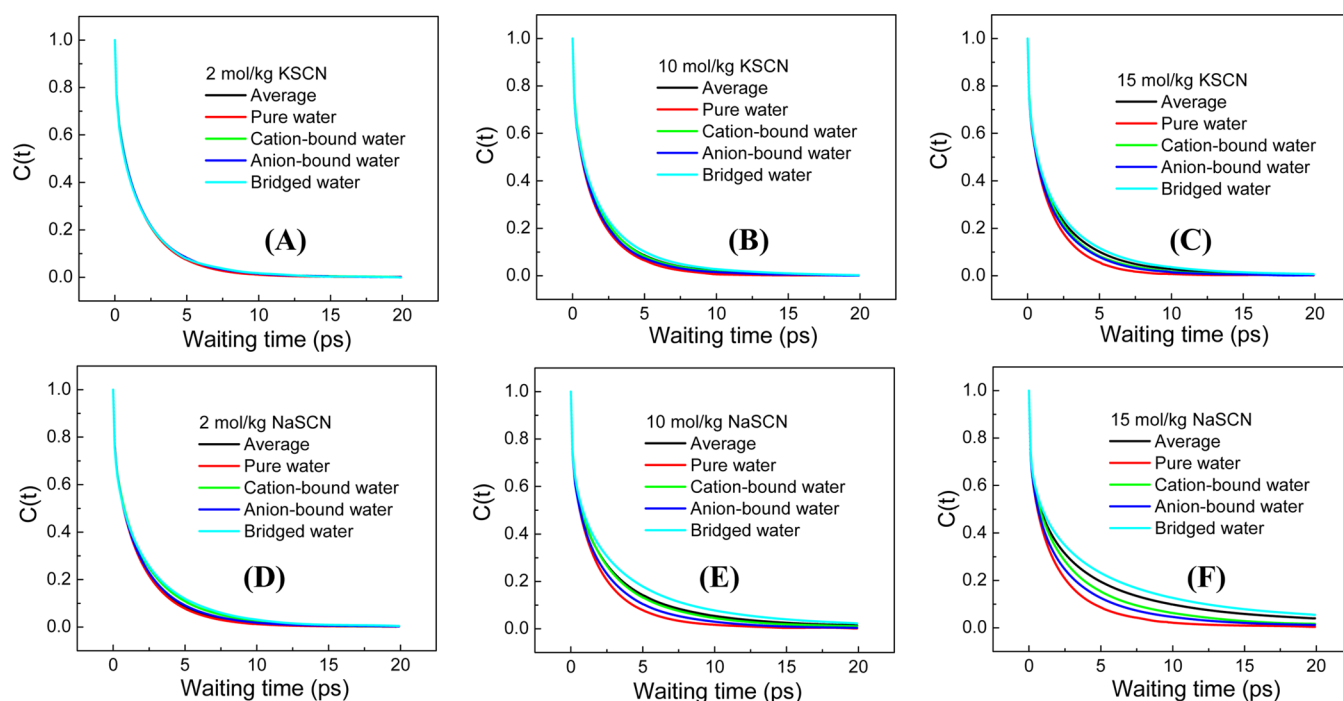


**Figure 7.** Reorientation correlation functions of water subspecies in aqueous solutions of (A) 2 mol/kg KSCN; (B) 10 mol/kg KSCN; (C) 15 mol/kg KSCN; (D) 2 mol/kg NaSCN; (E) 10 mol/kg NaSCN; and (F) 15 mol/kg NaSCN.

the correlation function. One important reason for us to do so is that the resident time of each species is comparable to or longer than its reorientation correlation.

Figure 7 displays the reorientation correlation functions of water subspecies in aqueous solutions of KSCN and NaSCN at the concentrations of 2, 10, and 15 mol/kg. The correlation time constant of single-exponential fit starting from 200 fs and the population of each species are listed in Table 2. In the KSCN solutions at various concentrations, the rotational behaviors of all water subspecies are generally similar (Figure 7A–C). At 2 mol/kg, all the water subspecies have essentially the same rotational time constant of 2.0–2.1 ps. The result implies that neither single  $\text{SCN}^-$  nor single  $\text{K}^+$  has noticeable

effects on the water reorientational motions. With the concentration increase to 15 mol/kg, the rotation of pure water slightly speeds up from 2.0 to 1.8 ps, and those of the cation- or anion-bound water molecules remain the same as in the 2 mol/kg solution. The bridged water molecules slow down about 25% from 2.1 to 2.6 ps. The slowdown is probably caused by the geometric confinements rather than the direct ion/water interactions which have negligible effects on the water rotations as discussed above. At higher concentrations, more and bigger ion clusters form, and the bridged water molecules have larger chances to be “locked” by more than one pair of ions.

In the NaSCN solutions (Figure 7D–F), situations are different from in the KSCN solutions. At 2 mol/kg, the rotation of  $\text{Na}^+$ -bound water molecules is about 20% slower than that of pure water. This slowdown can be attributed to the direct stronger  $\text{Na}^+$ /water interaction which probably leads to a larger rotational energy barrier, since in the KSCN solution of the same concentration neither  $\text{SCN}^-$  nor  $\text{K}^+$  of which the direct interaction with water is weaker than the  $\text{Na}^+$ /water interaction can affect the water dynamics. The rotation of bridged water molecules is even slower, about 30% slower than that of the pure water. Our MD simulations (Figure 8) show that the concentrations of ion clusters (including pairs) are similar in KSCN and NaSCN, and in fact the concentrations of clusters with more than two ions are larger in the KSCN solutions than in the NaSCN solutions. It is therefore unlikely that the slower dynamics of the bridged water than the  $\text{Na}^+$ -bound water in the 2 mol/kg NaSCN solution is caused by more geometric confinements for the bridged species, provided that the dynamics of both  $\text{K}^+$ -bound and bridged water in the 2 mol/kg KSCN solution are the same. A very likely reason is that the stronger  $\text{Na}^+/\text{SCN}^-$  interaction (than the  $\text{K}^+/\text{SCN}^-$  interaction) can further slow down the rotation of water between them, in addition to the  $\text{Na}^+$ /water interaction. It is interesting to note that even the rotation of  $\text{SCN}^-$ -bound water in the

**Table 2.** Correlation Time Constant of Single-Exponential Fit Starting from 200 fs and the Population (in Parentheses) of Each Species from the MD Simulations

	2 M KSCN	10 M KSCN	15 M KSCN	2 M NaSCN	10 M NaSCN	15 M NaSCN
average water	2.1	2.2	2.3	2.2	2.9	3.6
pure water	2.0 (58%)	1.9 (16%)	1.8 (8%)	2.1 (57%)	2.1 (11%)	2.2 (5%)
cation-bound water	2.1 (15%)	2.1 (16%)	2.1 (11%)	2.5 (14%)	2.8 (10%)	3.1 (7%)
anion-bound water	2.1 (20%)	2.0 (25%)	2.1 (20%)	2.3 (22%)	2.5 (27%)	2.7 (23%)
bridged water	2.1 (7%)	2.4 (43%)	2.6 (61%)	2.7 (7%)	3.5 (51%)	4.2 (66%)
average $\text{SCN}^-$	2.3	4.1	5.2	2.7	6.6	22
hydrated $\text{SCN}^-$	2.1 (36%)	2.3 (3%)	2.1 (1%)	2.3 (60%)	3.2 (7%)	5.3 (2%)
cation-bound $\text{SCN}^-$	2.4 (64%)	4.3 (97%)	5.2 (99%)	3.4 (40%)	7.0 (93%)	22 (98%)

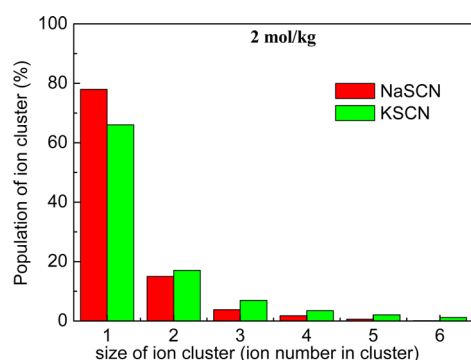


**Figure 8.** Concentrations of ion species in 2 mol/kg NaSCN and KSCN aqueous solutions.

NaSCN solution is also a little slower than that of pure water, different from that in the 2 M KSCN solution. This is probably because during the accumulation of the correlation function, the  $\text{SCN}^-$ -bound water has some chance to evolve into the  $\text{Na}^+$ -bound or bridged water of which the rotational dynamics are slower, but another explanation that the existence of  $\text{Na}^+$  can affect waters more than one solvation layer away cannot be completely excluded.

With the concentration increase, the rotational dynamics of the bridged water molecules slow down. At 15 mol/kg, the rotation of the bridged water is about 56% slower than at 2 mol/kg. This can also be explained in a way similar to that for the KSCN solution. At higher concentrations, the bridged water molecules have larger chances to directly interact with more than two ions (see Figure 9). In addition to more geometric

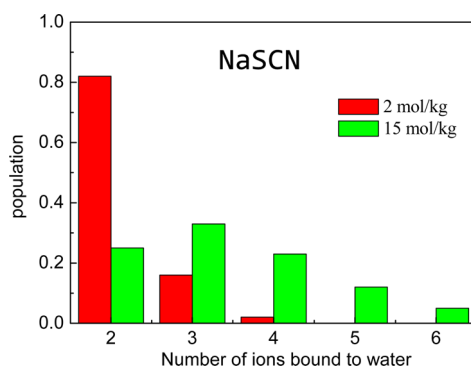


**Figure 9.** Populations of bridged-water species with different numbers of ions of 2 and 15 mol/kg NaSCN aqueous solutions.

confinements resulting from the ion clustering, the bridged water molecules experience more  $\text{Na}^+$ /water and  $\text{Na}^+/\text{SCN}^-$  interactions because more  $\text{Na}^+$  and  $\text{SCN}^-$  are present in their first solvation shells. According to the literature,<sup>49–51</sup> the water rotational mobility is closely related to the available volume and potential partners around the central water in the hydrogen bond exchanging process. More geometric confinements result in smaller available volume and fewer potential partners and therefore slow down the rotation. More water/ion interactions result in more total binding energy (higher rotational barrier), which will also slow down the water rotation. All these factors slow down the bridged water dynamics and therefore the slowdown amplitude in the NaSCN solutions is larger than in the KSCN solutions where the direct  $\text{K}^+$ /water or  $\text{K}^+/\text{SCN}^-$  interaction does not affect the water rotation. The rotation of

cation- or anion-bound water molecules also slows down with the increase of concentration. This can be explained in a way similar to that for the slower rotation of  $\text{SCN}^-$ -bound water in the 2 mol/kg NaSCN solution.

In summary, the calculated cation and concentration-dependent water reorientational dynamics are qualitatively in agreement with the experimental observations: water rotations are slower in a MSCN ( $M = \text{Li}, \text{Na}, \text{and K}$ ) solution at a higher concentration with a smaller cation. The calculations also show that such dynamical changes are the sum results of ion clustering and direct cation/water interactions.

**3.4.2. Reorientational Dynamics of  $\text{SCN}^-$  Anions.** The cation effect on the rotational dynamics of  $\text{SCN}^-$  is more pronounced than that on the water dynamics in the MD simulations. Figure 10 displays the reorientation correlation functions of  $\text{SCN}^-$  subspecies in aqueous solutions of KSCN and NaSCN at the concentrations of 2, 10, and 15 mol/kg. The correlation time constant of single-exponential fit starting from 200 fs and the population of each species are listed in Table 2. At 2 mol/kg, the rotation of  $\text{K}^+$ -bound  $\text{SCN}^-$  is comparable to that of the hydrated species with a time constant 2.4 ps. The rotation of the  $\text{Na}^+$ -bound  $\text{SCN}^-$  is obviously slower, with a time constant 3.4 ps. This is probably because the stronger  $\text{SCN}^-/\text{Na}^+$  interaction results in a larger rotational energy barrier. The longer  $\text{Na}^+/\text{SCN}^-$  pairing residence time (mathematically defined in our previous publication<sup>34</sup>) because of the stronger interaction can also be a reason for the observed slower rotation. At 2 mol/kg, in the NaSCN solution the residence times of  $\text{Na}-\text{S}(\text{SCN})$  and  $\text{Na}-\text{N}(\text{SCN})$  are respectively 13.7 and 16.2 ps. The corresponding values are 13.0 and 8.9 ps for the KSCN solution. The  $M-\text{S}$  residence times are similar for both cations. However, the  $M-\text{N}$  residence time is significantly shorter for  $\text{K}^+$ . Because the portions of  $M-\text{N}$  (out of the sum of  $M-\text{N} + M-\text{S}$ ) are more than 40% in both solutions, it is conceivable that the longer  $\text{Na}-\text{N}$  residence time can lead to a longer  $\text{SCN}^-$  rotational time. At higher concentrations, the rotations of both  $\text{K}^+$ - and  $\text{Na}^+$ -bound  $\text{SCN}^-$  anions become slower, but the slowdown amplitude in the NaSCN solutions is much more salient than in the KSCN solutions. At 15 mol/kg, the rotational time constant of  $\text{K}^+$ -bound  $\text{SCN}^-$  is 5.2 ps, but that of the  $\text{Na}^+$ -bound  $\text{SCN}^-$  is about 4 times longer, 22 ps. At this concentration, the first solvation shells of most  $\text{SCN}^-$  have more than one cation and most of these ions interconnect with each other, forming clusters in both KSCN and NaSCN solutions. The ion clustering can result in two effects which can slow down the rotation of  $\text{SCN}^-$ : (1) geometric confinements; and (2) more cation/anion interactions (coordinate number). Similar to that discussed above, the first effect can probably also result in a smaller available volume and fewer potential rotational partners, and the second effect can result in a higher rotational barrier. The geometric confinements mainly because of the close packing of cations and anions of the clusters exist for both KSCN and NaSCN solutions, but the  $\text{K}^+/\text{SCN}^-$  interaction is weaker than the  $\text{Na}^+/\text{SCN}^-$  solutions. If we assume that the rotational activation energy of  $\text{SCN}^-$  is approximately proportional to the cation/anion interaction strength, the slowdown of  $\text{SCN}^-$  rotation will roughly scale exponentially with the number of cation/anion interactions a  $\text{SCN}^-$  can experience. Therefore, in bigger clusters, the  $\text{Na}^+$ -bound  $\text{SCN}^-$  should slow down more than the  $\text{K}^+$ -bound species does.

In summary, similar to those of water molecules, the calculated rotational dynamic changes of  $\text{SCN}^-$  are also

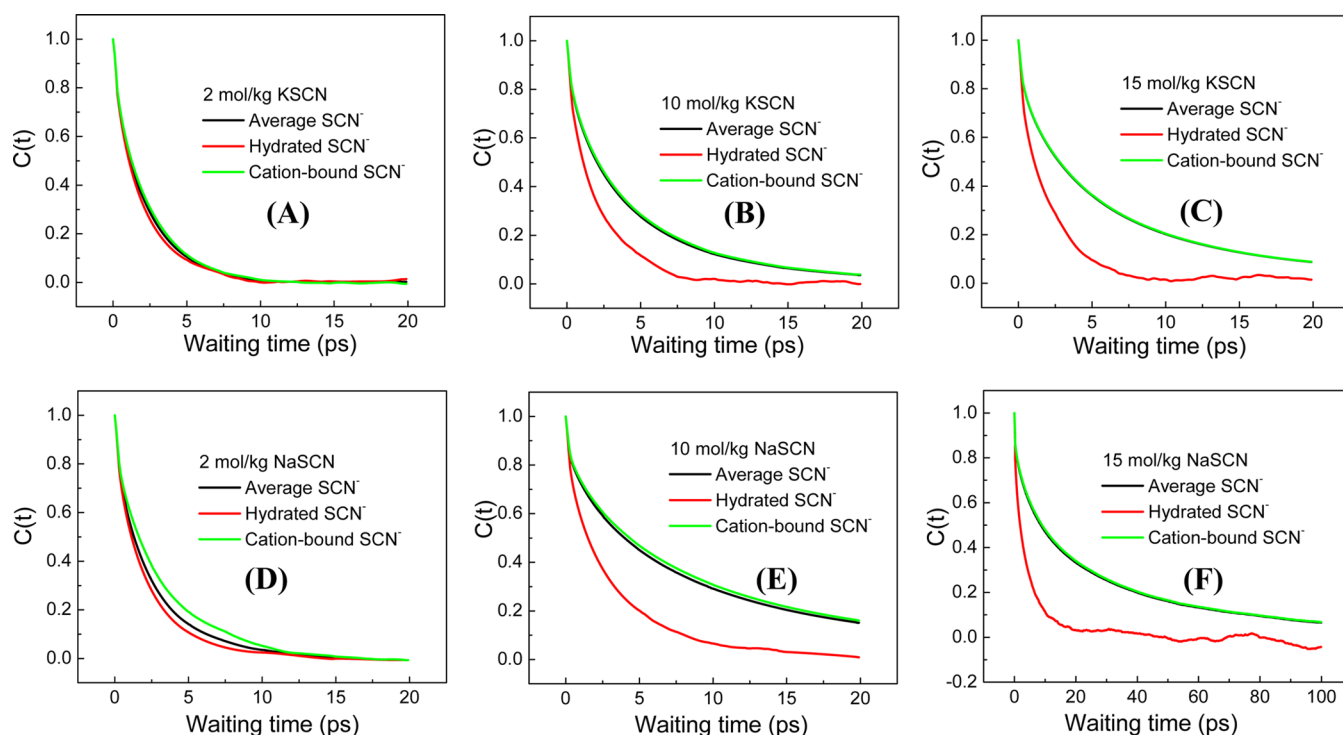


**Figure 10.** Reorientation correlation functions of  $\text{SCN}^-$  subspecies in aqueous solutions of (A) 2 mol/kg KSCN; (B) 10 mol/kg KSCN; (C) 15 mol/kg KSCN; (D) 2 mol/kg NaSCN; (E) 10 mol/kg NaSCN; and (F) 15 mol/kg NaSCN.

qualitatively consistent with the experimental observations. The experimentally observed concentration and cation dependences are reproduced very well by the simulations, but obviously the agreements are not at the quantitative level because many of the experimental and calculated rotational time constants are quite different.

We also conducted MD simulations on the LiSCN and CsSCN solutions. The results of CsSCN are very similar to those of KSCN (see Figure S12 in the Supporting Information). The results of LiSCN are similar to those of NaSCN, but opposite to the experimental results, the water rotations in the LiSCN solutions are slightly faster than those of NaSCN solutions (see Figure S12 in the Supporting Information). One possible reason for the discrepancy between experiments and theory is that the current force field used cannot well describe the interaction of  $\text{Li}^+$ –water, because  $\text{Li}^+$  has a very large charge density (largest in our objective cations). From the work in our previous publication<sup>34</sup> we also found a similar trend with the nonpolarizable models: both  $\text{F}^-$  and  $\text{Li}^+$  are difficult to describe with the nonpolarizable models. The polarizable and charge-transfer effects may be more important for the ions with high charge densities. The simulations including the polarizable effect (both water and ion are polarizable) are undergoing in our group.

**3.4.3. Single-Exponential and Biexponential Decays.** In experiments, we observed that, at high concentrations ( $\geq 10$  mol/kg), the rotational decays of water molecules in the  $\text{Li}^+$  and  $\text{Na}^+$  solutions cannot be described well with single-exponential decays. The non-single-exponential decay is not as obvious for the water rotations in the KSCN and CsSCN solutions or the  $\text{SCN}^-$  rotations in all solutions. We attribute the non-single-exponential decays to the distinct rotational dynamics of cation-affected water molecules and other water molecules of similar populations and possible non-single-

exponential decays of the cation-affected water species. The MD simulations provide some insights into some aspects of this problem. The calculations show that the rotational dynamics of all water and  $\text{SCN}^-$  species are not rigorously single-exponential decays. In addition, in the concentrated NaSCN solutions, e.g., 15 mol/kg, the water molecules can be roughly separated into two species: 66% is the bridged water with a rotational time constant 4.2 ps, and 34% is the rest with an average rotational time constant  $\sim 2.7$  ps. A similar population ratio of these two types of water molecules is also found in the KSCN solution, but the rotational time constants of these water molecules are very close to each other in the KSCN solution. This is consistent with the experimental observation that the nonexponential behavior is more pronounced in the NaSCN solutions. For the  $\text{SCN}^-$  anions, at high concentrations, most of them form cation-bound species in both KSCN and NaSCN solutions, and therefore the overall  $\text{SCN}^-$  rotations resemble those of the cation-bound species. This also explains why the nonexponential behavior is not as obvious for the  $\text{SCN}^-$  rotations. However, we want to emphasize here that the above explanations based only on a few not-well-defined subspecies are very approximate. In general, we believe that the overall rotational dynamics experimentally observed are the sum of all subspecies in the solution. Whether the dynamics can be phenomenologically described with a single-exponential decay depends on the population and dynamics of each subspecies which requires detailed quantitative calculations.

## 4. CONCLUDING REMARKS

In this work, through measuring the waiting-time-dependent rotational anisotropies of  $\text{SCN}^-$  anions and water molecules in alkali thiocyanate ( $\text{XSCN}$ ,  $\text{X} = \text{Li}, \text{Na}, \text{K}, \text{Cs}$ ) aqueous solutions at various concentrations with ultrafast infrared spectroscopy, we found that the nature of cations can significantly affect the



reorientational motions of both water molecules and  $\text{SCN}^-$  anions. The dynamics are slower in a solution with a smaller cation. The reorientational time constants follow the order of  $\text{Li}^+ > \text{Na}^+ > \text{K}^+ \simeq \text{Cs}^+$ . The changes of rotational time constants of  $\text{SCN}^-$  at various concentrations scale well with the changes of solution viscosity, but those of water molecules do not. In addition, the concentration-dependent amplitudes of dynamical changes are much more significant in the  $\text{Li}^+$  and  $\text{Na}^+$  solutions than those in the  $\text{K}^+$  and  $\text{Cs}^+$  solutions. Further investigations on the systems with the ultrafast vibrational energy exchange method and molecular dynamics simulations provide an explanation for the observations: the observed rotational dynamics are the balanced results of ion clustering and cation/anion/water direct interactions. In all solutions at high concentrations ( $>5$  M), substantial amounts of ions form clusters. The structural inhomogeneity in the solutions leads to distinct rotational dynamics of water and anions. The strong interactions of  $\text{Li}^+$  and  $\text{Na}^+$  because of their relatively large charge densities with water molecules and  $\text{SCN}^-$  anions, in addition to the likely geometric confinements because of ion clustering, substantially slow down the rotations of  $\text{SCN}^-$  anions and water molecules inside the ion clusters. The interactions of  $\text{K}^+$  and  $\text{Cs}^+$  with water or  $\text{SCN}^-$  are much weaker. The rotations of water molecules inside ion clusters of  $\text{K}^+$  and  $\text{Cs}^+$  solutions are not significantly different from those of other water species so that the experimentally observed rotational relaxation dynamics are only slightly affected by the ion concentrations.

## ■ ASSOCIATED CONTENT

### ● Supporting Information

Supporting figures and data about FTIR spectra, anisotropy data, and vibrational energy transfer analyses. This material is available free of charge via the Internet at <http://pubs.acs.org>.

## ■ AUTHOR INFORMATION

### Corresponding Author

\*E-mail: junrong@rice.edu (J.Z.), wzhuang@dicp.ac.cn (W.Z.).

### Notes

The authors declare no competing financial interest.

## ■ ACKNOWLEDGMENTS

This material is based upon work supported by the Welch foundation under Award No. C-1752, and the Air Force Office of Scientific Research under AFOSR Award No. FA9550-11-1-0070. J.R.Z. also thanks the David and Lucile Packard Foundation for a Packard fellowship. W.Z. gratefully acknowledges the support of the NSFC QingNian Grant 21003117, NSFC key Grant 21033008, and Science and Technological Ministry of China Grant 2011YQ09000505.

## ■ REFERENCES

- (1) Leberman, R.; Soper, A. K. Effect of High-Salt Concentrations on Water-Structure. *Nature* **1995**, *378*, 364–366.
- (2) Winter, B.; Faubel, M. Photoemission from Liquid Aqueous Solutions. *Chem. Rev.* **2006**, *106*, 1176–1211.
- (3) Mason, P. E.; Neilson, G. W.; Dempsey, C. E.; Barnes, A. C.; Cruickshank, J. M. The Hydration Structure of Guanidinium and Thiocyanate Ions: Implications for Protein Stability in Aqueous Solution. *Proc. Natl. Acad. Sci. U.S.A.* **2003**, *100*, 4557–4561.
- (4) Smith, J. D.; Saykally, R. J.; Geissler, P. L. The Effects of Dissolved Halide Anions on Hydrogen Bonding in Liquid Water. *J. Am. Chem. Soc.* **2007**, *129*, 13847–13856.
- (5) Tielrooij, K. J.; Garcia-Araez, N.; Bonn, M.; Bakker, H. J. Cooperativity in Ion Hydration. *Science* **2010**, *328*, 1006–1009.
- (6) Doyle, D. A.; Cabral, J. M.; Pfuetzner, R. A.; Kuo, A. L.; Gulbis, J. M.; Cohen, S. L.; Chait, B. T.; MacKinnon, R. The Structure of the Potassium Channel: Molecular Basis of  $\text{K}^+$  Conduction and Selectivity. *Science* **1998**, *280*, 69–77.
- (7) Marcus, Y.; Hefter, G. Ion Pairing. *Chem. Rev.* **2006**, *106*, 4585–4621.
- (8) Cappa, C. D.; Smith, J. D.; Wilson, K. R.; Messer, B. M.; Gilles, M. K.; Cohen, R. C.; Saykally, R. J. Effects of Alkali Metal Halide Salts on the Hydrogen Bond Network of Liquid Water. *J. Phys. Chem. B* **2005**, *109*, 7046–7052.
- (9) Kunz, W. Specific Ion Effects in Colloidal and Biological Systems. *Curr. Opin. Colloid Interface Sci.* **2010**, *15*, 34–39.
- (10) Hofmeister, F. Zur Lehre Von der Wirkung der Salze. *Arch. Exp. Natur. Pharmacol.* **1888**, *24*, 247–260.
- (11) Collins, K. D.; Washabaugh, M. W. The Hofmeister Effect and the Behavior of Water at Interfaces. *Q. Rev. Biophys.* **1985**, *18*, 323–422.
- (12) Cacace, M. G.; Landau, E. M.; Ramsden, J. J. The Hofmeister Series: Salt and Solvent Effects on Interfacial Phenomena. *Q. Rev. Biophys.* **1997**, *30*, 241–277.
- (13) Zhang, Y. J.; Cremer, P. S. Interactions between Macromolecules and Ions: the Hofmeister Series. *Curr. Opin. Chem. Biol.* **2006**, *10*, 658–663.
- (14) Zhang, Y. J.; Cremer, P. S. Chemistry of Hofmeister Anions and Osmolytes. In *Annual Review of Physical Chemistry*; Annual Reviews: Palo Alto, CA, 2010; Vol. 61; pp 63–83.
- (15) Frank, H. S.; Wen, W. Y. Structural Aspects of Ion-Solvent Interaction in Aqueous Solutions - a Suggested Picture of Water Structure. *Discuss. Faraday Soc.* **1957**, 133–140.
- (16) Marcus, Y. Effect of Ions on the Structure of Water: Structure Making and Breaking. *Chem. Rev.* **2009**, *109*, 1346–1370.
- (17) Gurney, R. W. *Ionic Processes in Solution*; McGraw-Hill: New York, 1953.
- (18) Omta, A. W.; Kropman, M. F.; Woutersen, S.; Bakker, H. J. Negligible Effect of Ions on the Hydrogen-Bond Structure in Liquid Water. *Science* **2003**, *301*, 347–349.
- (19) Omta, A. W.; Kropman, M. F.; Woutersen, S.; Bakker, H. J. Influence of Ions on the Hydrogen-Bond Structure in Liquid Water. *J. Chem. Phys.* **2003**, *119*, 12457–12461.
- (20) Fayer, M. D.; Moilanen, D. E.; Wong, D.; Rosenfeld, D. E.; Fenn, E. E.; Park, S. Water Dynamics in Salt Solutions Studied with Ultrafast Two-Dimensional Infrared (2D IR) Vibrational Echo Spectroscopy. *Acc. Chem. Res.* **2009**, *42*, 1210–1219.
- (21) Park, S.; Moilanen, D. E.; Fayer, M. D. Water Dynamics - The Effects of Ions and Nanoconfinement. *J. Phys. Chem. B* **2008**, *112*, 5279–5290.
- (22) Park, S.; Fayer, M. D. Hydrogen Bond Dynamics in Aqueous NaBr Solutions. *Proc. Natl. Acad. Sci. U.S.A.* **2007**, *104*, 16731–16738.
- (23) Tielrooij, K. J.; van der Post, S. T.; Hunger, J.; Bonn, M.; Bakker, H. J. Anisotropic Water Reorientation around Ions. *J. Phys. Chem. B* **2011**, *115*, 12638–12647.
- (24) Bian, H. T.; Li, J. B.; Zhang, Q.; Chen, H. L.; Zhuang, W.; Gao, Y. Q.; Zheng, J. R. Ion Segregation in Aqueous Solutions. *J. Phys. Chem. B* **2012**, *116*, 14426–14432.
- (25) van der Post, S. T.; Bakker, H. J. The Combined Effect of Cations and Anions on the Dynamics of Water. *Phys. Chem. Chem. Phys.* **2012**, *14*, 6280–6288.
- (26) Giammanco, C. H.; Wong, D. B.; Fayer, M. D. Water Dynamics in Divalent and Monovalent Concentrated Salt Solutions. *J. Phys. Chem. B* **2012**, *116*, 13781–13792.
- (27) Bakker, H. J. Structural Dynamics of Aqueous Salt Solutions. *Chem. Rev.* **2008**, *108*, 1456–1473.
- (28) Chen, A. A.; Pappu, R. V. Quantitative Characterization of Ion Pairing and Cluster Formation in Strong 1:1 Electrolytes. *J. Phys. Chem. B* **2007**, *111*, 6469–6478.



- (29) Hassan, S. A. Computer Simulation of Ion Cluster Speciation in Concentrated Aqueous Solutions at Ambient Conditions. *J. Phys. Chem. B* **2008**, *112*, 10573–10584.
- (30) Bian, H. T.; Wen, X. W.; Li, J. B.; Chen, H. L.; Han, S.; Sun, X. Q.; Song, J.; Zhuang, W.; Zheng, J. R. Ion Clustering in Aqueous Solutions Probed with Vibrational Energy Transfer. *Proc. Natl. Acad. Sci. U.S.A.* **2011**, *108*, 4737–4742.
- (31) Bian, H. T.; Chen, H. L.; Li, J. B.; Wen, X. W.; Zheng, J. R. Nonresonant and Resonant Mode-Specific Intermolecular Vibrational Energy Transfers in Electrolyte Aqueous Solutions. *J. Phys. Chem. A* **2011**, *115*, 11657–11664.
- (32) Li, J.; Bian, H.; Wen, X.; Chen, H.; Yuan, K.; Zheng, J. Probing Ion/Molecule Interactions in Aqueous Solutions with Vibrational Energy Transfer. *J. Phys. Chem. B* **2012**, *116*, 12284–12294.
- (33) Li, J. B.; Bian, H. T.; Chen, H. L.; Wen, X. W.; Hoang, B. T.; Zheng, J. R. Ion Association in Aqueous Solutions Probed through Vibrational Energy Transfers among Cation, Anion, and Water Molecules. *J. Phys. Chem. B* **2013**, *117*, 4274–4283.
- (34) Zhang, Q.; Wen, J.; Bian, H. T.; Gao, Y. Q.; Zheng, J. R.; Zhuang, W. Microscopic Origin of the Deviation from Stokes-Einstein Behavior Observed in Dynamics of the KSCN Aqueous Solutions: A MD Simulation Study. *J. Phys. Chem. A* **2013**, *117*, 2992–3004.
- (35) Einstein, A. The Motion of Elements Suspended in Static Liquids as Claimed in the Molecular Kinetic Theory of Heat. *Ann. Phys.-Berlin* **1905**, *17*, 549–560.
- (36) Sturlaugson, A. L.; Fruchey, K. S.; Lynch, S. R.; Aragon, S. R.; Fayer, M. D. Orientational and Translational Dynamics of Polyether/Water Solutions. *J. Phys. Chem. B* **2010**, *114*, 5350–5358.
- (37) Akers, C.; Peterson, S. W.; Willett, R. D. A Refinement of Crystal Structure of Kscn. *Acta Crystallogr. Sect. B: Struct. Crystallogr. Chem.* **1968**, *B 24*, 1125–1126.
- (38) Bian, H. T.; Wen, X. W.; Li, J. B.; Zheng, J. R. Mode-Specific Intermolecular Vibrational Energy Transfer. II. Deuterated Water and Potassium Selenocyanate Mixture. *J. Chem. Phys.* **2010**, *133*, 034505.
- (39) Bian, H. T.; Li, J. B.; Wen, X. W.; Zheng, J. R. Mode-Specific Intermolecular Vibrational Energy Transfer. I. Phenyl Selenocyanate and Deuterated Chloroform Mixture. *J. Chem. Phys.* **2010**, *132*, 184505.
- (40) Ponder, J. W.; Richards, F. M. An Efficient Newton-Like Method for Molecular Mechanics Energy Minimization of Large Molecules. *J. Comput. Chem.* **1987**, *8*, 1016–1024.
- (41) Collins, K. D. Charge Density-Dependent Strength of Hydration and Biological Structure. *Biophys. J.* **1997**, *72*, 65–76.
- (42) Sathaiah, S.; Sarin, V. N.; Bist, H. D. Vibrational Studies of the Structural Phase-Transition in Cesium Thiocyanate. *J. Phys.: Condens. Matter* **1989**, *1*, 7829–7841.
- (43) Aliev, A. R.; Gadzhiev, A. Z. Raman Spectra and Vibrational Relaxation in Molten Thiocyanates. *J. Mol. Liq.* **2003**, *107*, 59–67.
- (44) Baddiel, C. B.; Janz, G. J. Molten Thiocyanates: Raman Spectra and Structure. *Trans. Faraday Soc.* **1964**, *60*, 2009–2012.
- (45) Smith, D. W. Ionic Hydration Enthalpies. *J. Chem. Educ.* **1977**, *54*, 540–542.
- (46) Yamada, Y.; Watanabe, T. The Phase Transition of Crystalline Potassium Thiocyanate, Kscn 0.2. X-Ray Study. *Bull. Chem. Soc. Jpn.* **1963**, *36*, 1032–1037.
- (47) Vanrooyen, P. H.; Boeyens, J. C. A. Sodium Thiocyanate. *Acta Crystallogr. Sect. B: Struct. Sci.* **1975**, *31*, 2933–2934.
- (48) Irving, M. A.; Elcombe, M. M.; Smith, T. F. Neutron-Diffraction Studies of Cscn above Room-Temperature. *Aust. J. Phys.* **1985**, *38*, 85–95.
- (49) Laage, D.; Hynes, J. T. On the Molecular Mechanism of Water Reorientation. *J. Phys. Chem. B* **2008**, *112*, 14230–14242.
- (50) Laage, D.; Stirnemann, G.; Hynes, J. T. Why Water Reorientation Slows without Iceberg Formation around Hydrophobic Solutes. *J. Phys. Chem. B* **2009**, *113*, 2428–2435.
- (51) Sterpone, F.; Stirnemann, G.; Hynes, J. T.; Laage, D. Water Hydrogen-Bond Dynamics around Amino Acids: The Key Role of Hydrophilic Hydrogen-Bond Acceptor Groups. *J. Phys. Chem. B* **2010**, *114*, 2083–2089.